Journal of Thrombosis and Haemostasis, **8**: 2789–2799 DOI: 10.1111/j.1538-7836.2010.04075.x

ORIGINAL ARTICLE

The soluble form of urokinase receptor promotes angiogenesis through its Ser^{88}-Arg-Ser-Arg-Tyr^{92} chemotactic sequence

K. BIFULCO,*[1] I. LONGANESI-CATTANI,*[1] M. GALA,* G. DI CARLUCCIO,* M. T. MASUCCI,* V. PAVONE,† L. LISTA,† C. ARRA,* M. P. STOPPELLI‡ and M. V. CARRIERO*

**Department of Experimental Oncology, National Cancer Institute of Naples; †Department of Chemistry, University of Naples 'Federico II'; and ‡Institute of Genetics and Biophysics 'Adriano Buzzati-Traverso', National Research Council, Naples, Italy*

To cite this article: Bifulco K, Longanesi-Cattani I, Gala M, Di Carluccio G, Masucci MT, Pavone V, Lista L, Arra C, Stoppelli MP, Carriero MV. The soluble form of urokinase receptor promotes angiogenesis through its Ser^{88}-Arg-Ser-Arg-Tyr^{92} chemotactic sequence. *J Thromb Haemost* 2010; **8**: 2789–99.

Summary. *Background:* The urokinase plasminogen activator receptor (u-PAR) focuses the proteolytic activity of the urokinase plasminogen activator (u-PA) on the endothelial cell surface, thus promoting angiogenesis in a protease-dependent manner. The u-PAR may exist in a glycophosphatidylinositol-anchored and in a soluble form (soluble u-PAR [Su-PAR]), both including the chemotactic Ser^{88}-Arg-Ser-Arg-Tyr^{92} internal sequence. *Objective:* To investigate whether Su-PAR may trigger endothelial cell signaling leading to new vessel formation through its chemotactic Ser^{88}-Arg-Ser-Arg-Tyr^{92} sequence. *Methods and Results:* In this study, the formation of vascular-like structures by human umbilical vein endothelial cells was assessed by using a matrigel basement membrane preparation. First, we found that Su-PAR protein promotes the formation of cord-like structures, and that this ability is retained by the isolated Ser^{88}-Arg-Ser-Arg-Tyr^{92} chemotactic sequence, the maximal effect being reached at 10 nmol L^{-1} SRSRY peptide (SRSRY). This effect is mediated by the $\alpha_v\beta_3$ vitronectin receptor, is independent of u-PA proteolytic activity, and involves the internalization of the G-protein-coupled formyl-peptide receptor in endothelial cells. Furthermore, exposure of human saphenous vein rings to Su-PAR or SRSRY leads to a remarkable degree of sprouting. Finally, we show that Su-PAR and SRSRY promote a marked response in angioreactors implanted into the dorsal flank of nude mice, retaining 91% and 66%, respectively, of the angiogenic response generated by a mixture of vascular endothelial growth factor and fibroblast growth factor type 2. *Conclusions:* Our results show a new protease-independent activity of Su-PAR that stimulates *in vivo* angiogenesis through its Ser^{88}-Arg-Ser-Arg-Tyr^{92} chemotactic sequence.

Keywords: angiogenesis, endothelial cell migration, formyl-peptide receptor, soluble urokinase receptor, vitronectin receptor.

Correspondence: Maria Vincenza Carriero, Department of Experimental Oncology, National Cancer Institute of Naples, via M. Semmola, 80131, Naples, Italy.
Tel.: +39 0815903569; fax: +39 0815903814.
E-mail: mariolinacarriero@yahoo.it

[1]These authors contributed equally to this work.

Received 20 January 2010, accepted 13 September 2010

Introduction

During new vessel formation, endothelial cells (ECs) degrade their basement membrane, migrate into the interstitial matrix and proliferate. An imbalance in this process contributes to numerous malignant, inflammatory, ischemic, infectious and immune disorders [1]. The process is dependent on signaling from soluble growth factors and their cognate receptors, integrins and matrix molecules, in a complex network of interactions. In particular, $\alpha_v\beta_3$ vitronectin receptor engagement promotes phosphorylation and activation of vascular endothelial growth factor (VEGF) receptor, thus enhancing the subsequent signaling [2]. Also, the proangiogenic effect of VEGF may be further increased by its ability to induce rapid activation of pro-urokinase to the urokinase plasminogen activator (u-PA) [3].

u-PA is a serine protease endowed with a clear-cut signaling ability, which may impact on angiogenesis by a variety of mechanisms, such as the control of matrix remodeling, the bioavailability of angiogenic factors, including VEGF, and the activation of pro-matrix metalloproteases [4,5]. Upon binding to its cell surface receptor (u-PAR), u-PA elicits a variety of cell responses, including proliferation and migration, both of which support angiogenesis [6,7]. Signaling occurs through the assembly of u-PAR in composite regulatory units with transmembrane receptors, such as formyl-peptide receptor (FPR) and FPR-like (FPRL)-1 G protein-coupled receptors (GPCRs), integrins and epidermal growth factor receptor [6–8].

u-PAR is a glycosylated glycosylphosphatidylinositol (GPI)-anchored protein [9,10] formed by three domains, DI, DII and DIII, connected by short linker regions [11]. The linker region

between DI and DII is a protease-sensitive region that retains chemotactic activity both *in vitro* and *in vivo* [12–15].

Enzymatic cleavage of the lipid anchor or alternative splicing generate truncated forms of u-PAR (soluble u-PAR [Su-PAR]), which are secreted into the extracellular milieu. Soluble forms of intact u-PAR or cleaved receptor (u-PARDII-DIII and u-PARDI) have been detected in tumor tissues and body fluids, and are associated with a poor prognosis [16–18].

X-ray studies have demonstrated the flexibility of the u-PAR domain organization [19,20]. The linker region between DI and DII is located on the external surface of u-PAR, and includes the Ser^{88}-Arg-Ser-Arg-Tyr^{92} sequence, which is chemotactically active, even in the form of an isolated SRSRY [14,15]. The flexibility of this region enables it to interact with a wide variety of ligands [20]. Also, u-PAR engagement with u-PA favors the exposure of the u-$PAR_{88–92}$ sequence, thus activating signaling. *In vitro*, Su-PAR or the u-PAR-derived SRSRY regulate the activity of chemokine receptors in an integrin-dependent manner [21]. SRSRY promotes cytoskeletal rearrangements and directional cell migration by binding to the G-protein-coupled high-affinity FPR [15]. Other receptors of the FPR family (FPRL-1 and FPRL-2) have been shown to respond to the same chemotactic sequence [12,14]. Upon binding to FPR, SRSRY triggers vitronectin receptor activation with an inside-out type of mechanism [15].

Given the abundance and the prognostic relevance of Su-PAR in cancer, we investigated the involvement of Su-PAR in neoangiogenesis by a direct mechanism. In this study, we present evidence that Su-PAR induces tube formation by human ECs, and that this effect is mediated by its chemotactic Ser^{88}-Arg-Ser-Arg-Tyr^{92} sequence. This proangiogenic effect is exerted through formyl-peptide and $\alpha_v\beta_3$ vitronectin receptors, both of which are known interactors of u-PAR. We found that the proangiogenic effect is reproducible on human vein rings, which show a remarkable degree of sprouting of ECs when exposed to Su-PAR or to the SRSRY. Finally, the proangiogenic abilities of Su-PAR and the SRSRY were confirmed *in vivo* by the use of matrigel-containing angioreactors implanted in nude mice.

Materials and methods

Peptide synthesis and purification

Peptides were synthesized by the solid-phase approach and purified as previously described [22]. Molecular masses were confirmed by mass spectrometry.

Cell culture

Human umbilical vein endothelial cells (HUVECs), used between the third to the seventh passage according to Arnaoutova and Kleinman [23], were grown in Eagle Basal Medium (EBM) supplemented with 4% fetal bovine serum (FBS), 0.1% gentamicin, 1 μg mL^{-1} hydrocortisone, 10 μg mL^{-1} epidermal growth factor and 12 μg mL^{-1} bovine brain extract (Cambrex, Bio Science, Walkersville, MD, USA). Mouse fibroblast LB6 cells, and mouse LB6 cells secreting human Su-PAR (LB6/hSu-PAR) were grown in Dulbecco's modified Eagle's medium (DMEM) supplemented with 10% FBS, 100 IU mL^{-1} penicillin and 50 μg mL^{-1} streptomycin [24]. Soluble human u-PAR was purified from the conditioned medium of mouse LB6/hSu-PAR cells and quantified by ELISA as previously described [25].

Tube formation in a non-contact coculture system

LB6 or LB6/hSu-PAR cells were grown to 80% confluence (1.5×10^5 cells per well) on 24-well plates, and kept serum-free for 12 h prior to the experiment. Growth factor-reduced matrigel (100 μL per well) (BD Pharmigen, Erembodegem, Belgium; cat. 356230) was allowed to polymerize on a polyester membrane in an intercup chamber. Subsequently, the intercup chamber was introduced into the wells filled with DMEM with or without 5 μg mL^{-1} rabbit polyclonal antibody, recognizing the u-$PAR_{84–95}$ sequence. HUVECs (4×10^4 cells per sample) were seeded on matrigel at 37 °C and 5% CO_2 for 18 h. To quantify tube formation, five random areas per well at × 100 magnification were imaged, and the number of tubes formed by cord-like structures exceeding 100 μm in length [26], measured with Axiovision 4.4 software (Carl Zeiss, Milan, Italy), was counted.

EC tube formation assay

The formation of vascular-like structures was assessed on matrigel as previously described [27], with minor modifications. HUVECs (4×10^4 cells per well) were suspended in 300 μL of prewarmed culture medium without FBS. Diluents or effectors were added to the cell suspension prior to seeding cells on matrigel-coated plates. Recombinant $DI_{1–87}$, $DIII_{184–284}$ or $DIIDIII_{88–284}$ (Calbiochem, Darmstadt, Germany) were employed at 10 nmol L^{-1}. Assays were carried out for 6 h or for the indicated times at 37 °C in humidified air with 5% CO_2, as previously described [23,27]. When indicated, cells were preincubated with 5 μg mL^{-1} of the indicated antibodies, or 1 μg mL^{-1} anti-human VEGF polyclonal antibody (Ab) neutralizing the biological activity of $VEGF_{165}$ and $VEGF_{121}$ (R&D Systems, Milan, Italy). Other experiments were performed with cells preincubated for 1 h at 37 °C with 10 μg mL^{-1} aprotinin serine protease inhibitor (Sigma-Aldrich, Milan, Italy). The net contribution of each effector in promoting tube formation was calculated as a percentage of tube-like structures counted in the absence of any angiogenic stimulus (EBM), considered as 100%. In the experiments performed on ECs pre-exposed to antibodies or supplements, the effect of each supplement and the contribution of each effector were calculated as percentages of the 100% basal level. Quantification of tube formation was performed as described above.

Motility assay

Cell migration assays were performed with Boyden chambers and 8-μm pore size polyvinylpyrrolidone-free polycarbonate

filters (Nucleopore, Concorezzo-Milan, Italy), as previously described [15]. Briefly, cells were detached and counted, and viable cells were seeded in the upper chamber at 7×10^4 cells per well in culture medium without FBS. The lower chamber was filled with culture medium without FBS, with or without 40 ng mL^{-1} $VEGF_{165}$ (BD Pharmigen), 1 nmol L^{-1} Su-PAR, 10 nmol L^{-1} *N*-formyl-Nle-Leu-Phe-Nle-Tyr-Lys (fMLF) (Sigma-Aldrich) or synthetic peptides at the indicated concentrations. Incubation was carried out for 4 h at 37 °C in humidified air with 5% CO_2. In some experiments, 5 μg mL^{-1} 399 anti-u-PAR Ab recognizing cleaved and uncleaved forms of Su-PAR [28] (American Diagnostica, Pfungstadt, Germany) or 5 μg mL^{-1} LM609 anti-$\alpha_v\beta_3$ mAb (Chemicon Millipore, Milan, Italy) was preincubated with the cell suspension for 1 h at 37 °C and maintained throughout the assay. Other experiments were performed with cells desensitized with 100 nmol L^{-1} SRSRY or 100 nmol L^{-1} fMLF for 1 h at 37 °C in humidified air with 5% CO_2. In all cases, at the end of the assay, the migrated cells on the lower filter surfaces were fixed with ethanol, stained with hematoxylin, and counted in 10 random fields per filter at × 200 magnification.

Fluorescence microscopy

HUVECs grown on glass slides to semiconfluence were preincubated with diluents, 100 nmol L^{-1} fMLF, 100 nmol L^{-1} SRSRY or 10 nmol L^{-1} Su-PAR for 30 min at 37 °C or for 60 min at 4 °C, and extensively rinsed with phosphate-buffered saline (PBS) or treated with acid (50 mmol L^{-1} glycine–HCl buffer, pH 3.0) for 5 min at room temperature to remove receptor-bound ligands [29]. Thereafter, cells were exposed to 10 nmol L^{-1} *N*-formyl-Nle-fluorescein or Leu-Phe-Nle-Tyr-Lys-fluorescein (Molecular Probes, San Giuliano Milanese, Milan, Italy) for 30 or 60 min at 4 °C or 37 °C, and analyzed with an LMS510 confocal microscope (Carl Zeiss) as previously described [22]. In a subset of experiments, HUVECs (1.5×10^5 cells per well) were subjected to the same treatments, and cell-associated fluorescence was measured with a Victor 3 fluorescence plate reader (Perkin Elmer, Monza, Milan, Italy).

Human venous ring cultures

Forthy-eight-well tissue culture-grade plates were covered with 200 μL of matrigel and allowed to gel for 30–45 min at 37 °C and 5% CO_2. Surgically removed human saphenous vein specimens were cut into 2–3-mm-long cross-sections, rinsed in EBM, placed on the matrigel-coated wells, covered with an additional 200 μL of matrigel, and allowed to gel for 30–45 min at 37 °C and 5% CO_2. The rings were cultured in 1 mL of complete growth medium. After 24 h of incubation, the medium was removed and replaced with 1 mL of culture medium without FBS, supplemented with 10 mg mL^{-1} gentamicin, with or without 40 ng mL^{-1} $VEGF_{165}$, 1 nmol L^{-1} Su-PAR or 10 nmol L^{-1} SRSRY. The medium was changed every 2 days. Rings were evaluated every day with a phase contrast microscope (Carl Zeiss) equipped with a digital camera. Quantification of capillary sprouting was assessed by measuring the length of at least 10 sprouts emerging from the venous ring (radii) and calculating, for each radius, the area of circular segment according to the formula: πr^2 90°/360°. To confirm the occurrence of ECs in ring sprouts, matrigel-containing venous rings and sprouts were embedded in OCT compound (Gentaur, Kampenhout, Belgium), and then sectioned and immunostained with anti-CD31 (BD Pharmingen). Nuclei were counterstained with 4′,6-diamidino-2-phenylindole.

In vivo *angiogenesis assay*

The DIVAA (Trevigen, Gaithersburg, MD, USA) assay kit was employed as a quantitative *in vivo* method for the assay of angiogenesis, as previously described [30]. Silicone cylinders of volume 20 μL (angioreactors) were filled with an extract containing extracellular matrix mixed with diluents, 12.5 ng of VEGF and 37.5 ng of fibroblast growth factor type 2 (FGF-2), 1 nmol L^{-1} Su-PAR or 10 nmol L^{-1} SRSRY. Two angioreactors were implanted subcutaneously in the dorsal region of each CD1 nude mouse. Fifteen days after the implantation, mice were killed, and angioreactors were removed. Then, the vessel-containing matrix was removed from the cylinders. Cells recovered by digestion with dispase were stained with fluorescein isothiocyanate (FITC)–lectin. ECs were quantified by fluorescence at 510 nm with 485 nm excitation, using a Victor 3 fluorimeter, according to the manufacturer's instructions.

Statistical analysis

The results are expressed as the means ± standard deviations of the number of the indicated determinations. Data were analyzed by one-way analysis of variance and *post hoc* Bonferroni's modified *t*-test for multiple comparisons. $P < 0.05$ was accepted as significant.

Results

Effect of Su-PAR on endothelial tube formation in a coculture assay

First, we investigated whether Su-PAR, secreted by living cells, affects endothelial tube formation in a non-contact coculture system. Wild-type mouse LB6 cells and mouse LB6 cells secreting human Su-PAR (LB6/hSu-PAR) were grown to confluence. For the coculture assay, HUVECs were plated on matrigel with the use of an intercup chamber, allowing them to be exposed to the LB6 secretion products. Formation of cord-like structures was monitored after 18 h of incubation. We found that LB6/hSu-PAR cells stimulated ECs to form tube-like structures (Fig. 1A). The number of tubes formed by cord-like structures exceeding 100 μm in length was three to four times higher in HUVECs cocultured with LB6/hSu-PAR cells than in HUVECs cocultured with LB6 cells. The addition of anti-u-$PAR_{84–95}$ Ab to the LB6/hSu-PAR cells reduced almost to basal levels the number of cord-like structures, suggesting

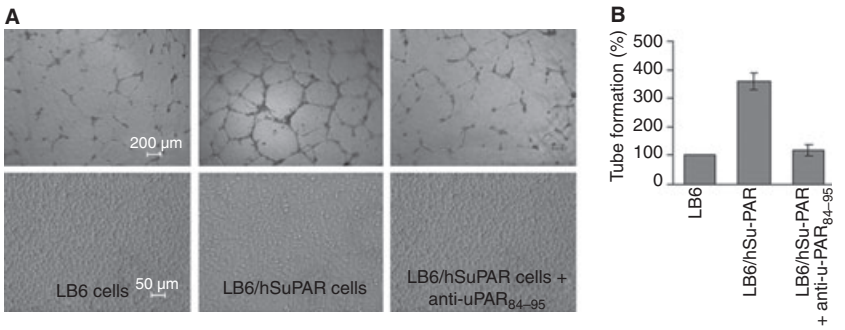

Fig. 1. Soluble urokinase plasminogen activator receptor (Su-PAR) promotes endothelial tube formation. Tube formation of human umbilical vein endothelial cells (HUVECs) cocultured for 18 h in a non-contact coculture system with mouse fibroblast wild-type LB6 or LB6/hSu-PAR cells. HUVECs plated on matrigel in an intercup chamber were layered onto LB6 or LB6/hSu-PAR cells in the presence or in the absence of anti-urokinase plasminogen activator receptor (u-PAR)$_{84–95}$ polyclonal antibody. (A) Representative pictures were taken with an inverted microscope. Original magnifications: × 50. (B) Quantization of tubes formed by cord-like structures exceeding 100 μm in length was calculated as a percentage of tubes formed by HUVECs plated on wild-type LB6 cells (considered as 100%). Data are expressed as the means ± standard deviations of two independent experiments performed in duplicate.

the involvement of the Ser^{88}-Arg-Ser-Arg-Tyr^{92} sequence in the proangiogenic effect of Su-PAR (Fig. 1A,B).

Dose-dependent and time-dependent effect of the Ser^{88}-Arg-Ser-Arg-Tyr^{92} u-PAR sequence on endothelial tube formation

We analyzed the ability of ECs to form cord-like structures on matrigel upon exposure to Su-PAR. HUVECs were plated on matrigel in the presence of the indicated effectors, and the appearance of tubular branches was observed after 6 h. For each experiment, we considered as 100% the baseline level of new formed cord-like structures assessed in the presence of matrigel alone. As a result, the number of tube-like structures exceeding 100 μm in length, counted in the absence of any effector, was 35 ± 10 per well. We found that 40 ng mL^{-1} VEGF$_{165}$ elicited a considerable response, rising to 236% over basal (Fig. 2A and Table 1). Interestingly, 1 nmol L^{-1} Su-PAR or 10 nmol L^{-1} recombinant DIIDIII$_{88–284}$ triggered appreciable endothelial tube formation (189% and 180%, respectively), whereas recombinant DI$_{1–87}$ or DIII$_{184–284}$, both of which lack the Ser^{88}-Arg-Ser-Arg-Tyr^{92} chemotactic sequence, were ineffective at 10 nmol L^{-1} (Table 1). The formation of tube-like structures induced by Su-PAR was attributable to its chemotactic Ser^{88}-Arg-Ser-Arg-Tyr^{92} sequence, as HUVECs failed to form tubes in the presence of 399 anti-u-PAR or anti-u-PAR$_{84–95}$ Abs (Table 1). Accordingly, SRSRY promoted capillary tube formation, whereas the control peptide ARARY was ineffective (Fig. 2A and Table 1).

We reasoned that u-PAR proximal partners may be shared among different cell types and, possibly, with the VEGF-dependent signaling pathway leading to angiogenesis. Therefore, we tested the possibility that u-PAR-dependent signaling may involve $\alpha_v\beta_3$. Remarkably, $\alpha_v\beta_3$ vitronectin receptor is required in this process, as ECs exposed to SRSRY or Su-PAR failed to form cord-like structures in the presence of anti-$\alpha_v\beta_3$ blocking mAb (Table 1).

To exclude the possibility that, under our conditions, traces of u-PA may promote proteolytic-dependent angiogenesis, the assay was also performed in the presence of the serine protease inhibitor aprotinin or 394 mAb (American Diagnostica), which blocks u-PA enzymatic activity. We found that, in the presence of blocking anti-u-PA mAb, the proangiogenic effects of Su-PAR or SRSRY were unchanged, suggesting the existence of a new, additional protease-independent role of u-PAR in angiogenesis (Table 1). Furthermore, the proangiogenic effect was not attributable to the cell releasing VEGF into the medium, because the addition of neutralizing anti-VEGF antibody to Su-PAR or SRSRY did not abrogate capillary tube formation (Table 1).

By a time-course experiment, we found that, as early as 2 h, 10 nmol L^{-1} SRSRY stimulated ECs to form cord-like structures, which continued to become more complex over the next 18 h (Fig. 2B). In ECs exposed to 10 nmol L^{-1} ARARY, tube formation was not observed, and cells remained sparse even at later times (Fig. 2C), supporting a specific effect of SRSRY on tube formation. The number of cord-like structures increased at early time points, whereas it did not change significantly between 6 and 24 h of incubation, peaking in both cases at 10 nmol L^{-1} (Fig. 2D).

Involvement of FPR in SRSRY signaling leading to tube formation

To gain further mechanistic insights into the SRSRY-dependent EC cord-like structures, the ability of ECs to migrate towards VEGF$_{165}$ or to a wide concentration range of SRSRY was assessed. We found that both VEGF and SRSRY elicited considerable dose-dependent HUVEC migration, reaching 231% and 180% of the basal cell migration, respectively, whereas ARARY did not exert any effect up to 10 μmol L^{-1} (Table 1 and Fig. 3). This ability was retained by Su-PAR (190%). Similarly to what was observed in the tube formation assays, SRSRY-induced EC migration was dose-dependent and peaked at 10 nmol L^{-1}; furthermore, it was abrogated by 399 anti-u-PAR Ab or by blocking anti-$\alpha_v\beta_3$ mAb, as well as by cell desensitization with

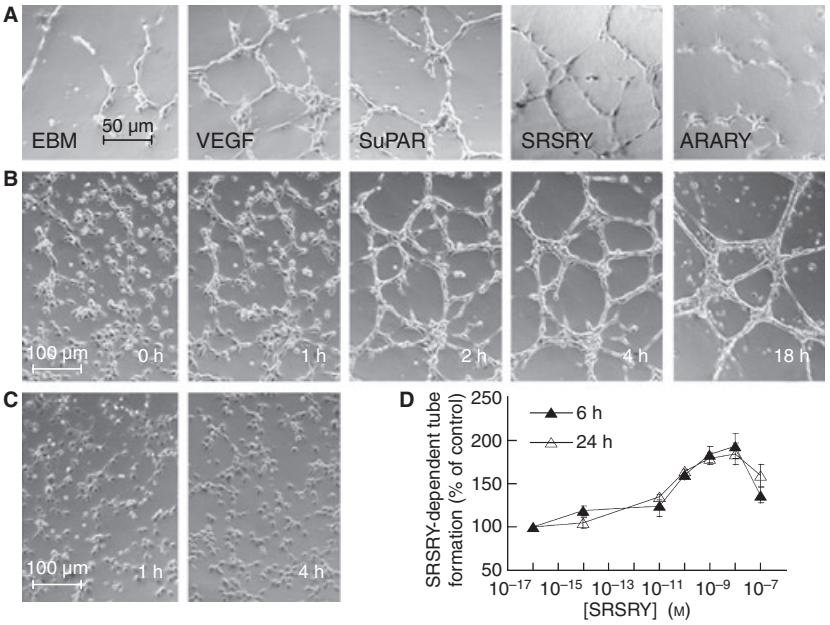

Fig. 2. The ability of soluble urokinase plasminogen activator receptor (Su-PAR) to promote tube formation is retained by SRSRY. (A) Human umbilical vein endothelial cells (HUVECs) were suspended in prewarmed culture medium without fetal bovine serum (FBS) (Eagle Basal Medium [EBM]), with or without 40 ng mL^{-1} vascular endothelial growth factor $(VEGF)_{165}$, 1 nmol L^{-1} Su-PAR, 10 nmol L^{-1} SRSRY or 10 nmol L^{-1} ARARY, and seeded on matrigel-coated plates for 6 h at 37 °C. Representative pictures were taken with an inverted microscope. Original magnifications: × 200. (B, C) Time course of HUVECs suspended in culture medium without FBS and seeded on matrigel-coated plates in the presence of 10 nmol L^{-1} SRSRY (B) or 10 nm ARARY (C). Representative images were captured at the indicated times. Original magnifications: × 100. (D) HUVECs, suspended in serum-free culture medium, were exposed to increasing concentration of SRSRY prior to seeding on matrigel for 6 or 24 h at 37 °C. Quantization of tube formation was calculated as a percentage of tubes, formed by cord-like structures exceeding 100 μm in length, counted in the absence of any angiogenic stimulus, considered as 100%. The data are expressed as the means ± standard deviations of three independent experiments performed in duplicate.

100 nmol L^{-1} SRSRY or 100 nmol L^{-1} fMLF (Fig. 3 and Table 1).

These findings raised the possibility that the molecular mechanisms underlying EC migration towards SRSRY are shared with those underlying tube formation in response to SRSRY. We have previously shown that: (i) u-PAR binds to FPRs through its Ser^{88}-Arg-Ser-Arg-Tyr^{92} sequence, thus promoting dose-dependent directional cell migration of HEK-293 human kidney cells; (ii) cell desensitization with an excess of fMLF abrogates u-PAR-dependent FPR activation; and (iii) SRSRY-triggered signaling is supported by cross-talk between FPR and the α_v chain of the vitronectin receptor [14,15].

To investigate whether FPR has a role in SRSRY-dependent endothelial tube formation, a subset of experiments was performed on ECs desensitized with an excess of fMLF or SRSRY and subsequently exposed to SRSRY. In ECs, the cord-like formation activity of Su-PAR and SRSRY was fully prevented by desensitization with fMLF, being 92% ± 3% and 95% ± 4%, respectively, of the basal level, taken as 100% (Table 1 and Fig. 4A). Similarly, both Su-PAR and SRSRY failed to trigger cord-like structure formation of SRSRY-desensitized ECs (Fig. 4A and Table 1). These findings indicate that FPR is a crucial mediator of the SRSRY-dependent response. To evaluate the direct binding of SRSRY to FPR, ECs were incubated with diluents, 100 nmol L^{-1} fMLF, 100 nmol L^{-1} SRSRY peptide or 10 nmol L^{-1} Su-PAR for 60 min, at 4 °C to avoid internalization, exposed to 10 nmol L^{-1} fMLF-fluorescein for an additional 60 min at 4 °C, and analyzed with a confocal microscope. As expected, FPR probed by its fluorescent agonist appeared to be mainly localized on the cell surface, as indicated by thin green fluorescent spots, which were dramatically reduced by pre-exposure of cells to fMLF (Fig. 4B) or by a short acid treatment (Fig. 4C). Both Su-PAR and SRSRY prevented binding of fMLF-fluorescein to FPR, indicating that u-PAR associates with FPR through its Ser^{88}-Arg-Ser-Arg-Tyr^{92} sequence (Fig. 4B). In response to agonist stimulation, many GPCRs, including FPR, are internalized [22,31]. To evaluate the effect of SRSRY on agonist-dependent FPR internalization, binding experiments were performed at 37 °C. As shown in Fig. 4D, upon exposure to fluorescent agonist, FPR appeared to be mainly internalized, with the appearance of fluorescent intracytoplasmic spots, which were undetectable in cells preincubated with an excess of non-fluorescent fMLF. These results were further confirmed by *z*-stack analysis of confocal images (Fig. S1). Interestingly, pre-exposure of cells to 10 nmol L^{-1} SRSRY or 1 nmol L^{-1} Su-PAR for 30 min at 37 °C strongly reduced agonist-dependent FPR internalization in all of the cells, again suggesting a mechanism in which SRSRY mimics fMLF-dependent FPR activation. To assess

Table 1 The ability of Soluble urokinase plasminogen activator receptor (Su-PAR) to promote tube formation and directional cell migration is retained by the SRSRY

Preincubation	Effector	Tube formation (%)	Cell migration (%)
EBM	EBM[a]	100	100
	40 ng mL^{-1} VEGF	236 ± 14**	231 ± 5**
	1 nmol L^{-1} Su-PAR	189 ± 2**	190 ± 12**
	10 nmol L^{-1} $D1_{1–87}$	119 ± 5	
	10 nmol L^{-1} $D3_{184–284}$	80 ± 9	
	10 nmol L^{-1} $D2D3_{88–284}$	180 ± 9*	
	10 nmol L^{-1} SRSRY	188 ± 12**	170 ± 5**
	10 nmol L^{-1} ARARY	109 ± 6	105 ± 6
	10 nmol L^{-1} fMLF		216 ± 23*
5 μg mL^{-1} 399 u-PAR Ab	EBM	95 ± 3	90 ± 4
	1 nmol L^{-1} Su-PAR	97 ± 2	93 ± 7
	10 nmol L^{-1} SRSRY	102 ± 5	95 ± 8
5 μg mL^{-1} u-$PAR_{84–95}$ Ab	EBM	97 ± 2	98 ± 3
	1 nmol L^{-1} Su-PAR	118 ± 9	
	10 nmol L^{-1} SRSRY	102 ± 3	101 ± 7
5 μg mL^{-1} LM609 $\alpha_v\beta_3$ mAb	EBM	89 ± 5	93 ± 2
	40 ng mL^{-1} VEGF	92 ± 5	98 ± 5
	1 nmol L^{-1} Su-PAR	94 ± 8	92 ± 3
	10 nmol L^{-1} SRSRY	98 ± 4	95 ± 2
1 μg mL^{-1} VEGF Ab	EBM	98 ± 4	
	40 ng mL^{-1} VEGF	103 ± 5	
	1 nmol L^{-1} Su-PAR	159 ± 9*	
	10 nmol L^{-1} SRSRY	153 ± 4*	
5 μg mL^{-1} 394 u-PA mAb	EBM	102 ± 3	
	1 nmol L^{-1} Su-PAR	195 ± 8**	
	10 nmol L^{-1} SRSRY	183 ± 2**	
10 μg mL^{-1} aprotinin	EBM	98 ± 6	
	1 nmol L^{-1} Su-PAR	150 ± 8*	
100 nmol L^{-1} fMLF	EBM	93 ± 7	95 ± 5
	1 nmol L^{-1} Su-PAR	92 ± 3	99 ± 4
	10 nmol L^{-1} SRSRY	95 ± 4	97 ± 3
100 nmol L^{-1} SRSRY	EBM	90 ± 3	98 ± 6
	1 nmol L^{-1} Su-PAR	98 ± 4	97 ± 2
	10 nmol L^{-1} SRSRY	95 ± 1	90 ± 10

Ab, polyclonal antibody; EBM, Eagle Basal Medium; fMLF, *N*-formyl-Nle-Leu-Phe-Nle-Tyr-Lys; u-PAR, urokinase plasminogen activator; VEGF, vascular endothelial growth factor. Human umbilical vein endothelial cells preincubated with diluents (EBM), the indicated antibody or supplements for 1 h at 37 °C were seeded on matrigel for tube formation assays or in Boyden chambers for directional cell migration assays, in the presence or in the absence of the indicated effectors. Quantitative analysis of tube formation and cell migration was performed as described in Materials and methods. Data are the means ± standard deviations of three independent experiments performed in duplicate. Statistical significance with *P*-values was calculated against the control (EBM). *Statistical significance with $P < 0.05$ **Statistical significance with $P < 0.001$. [a]In all cases, the basal value (EBM) was taken as 100%, and all values were reported relative to this.

whether SRSRY itself causes FPR internalization, HUVECs were preincubated with 100 nmol L^{-1} fMLF, 10 nmol L^{-1} Su-PAR, 100 nmol L^{-1} SRSRY or 100 nmol L^{-1} ARARY at 37 °C, rinsed with PBS or acid-treated to remove receptor-bound ligands [29] and then exposed to 10 nmol L^{-1} fMLF-fluorescein at 4 °C for 60 min. Measurement of cell-associated fluorescence revealed that pre-exposure of cells to fMLF strongly reduced cell-associated fluorescence, in both untreated and acid-treated cells, whereas ARARY did not modify binding of fMLF-fluorescein to surfaces of either untreated or acid-treated cells. Similarly to fMLF, both SRSRY and Su-PAR prevented binding of fluorescent FPR agonist to surfaces of both acid-untreated and acid-treated cells (Fig. 4E), thus indicating that u-PAR effectively binds FPR and triggers its internalization.

Sprouting of cultured human saphenous vein rings exposed to SRSRY

To investigate whether the Ser^{88}-Arg-Ser-Arg-Tyr^{92} chemotactic sequence of u-PAR retains the ability to influence microvessel formation in a more complex environment, an *ex vivo* model of human saphenous vein rings was used. To this end, human saphenous vein rings of thickness 2–3 mm were embedded in matrigel and cultured for 5–7 days. In the presence of VEGF, vein rings exhibited capillary sprouting into the vessel lumen (not shown) and outwards, possibly because of the external VEGF gradient (Fig. 5). We found that both Su-PAR and SRSRY, although to different extents, increased capillary sprouting from the rings as compared with the control. The endothelial nature of sprout rings generated by Su-PAR was confirmed by immunostaining of the matrigel

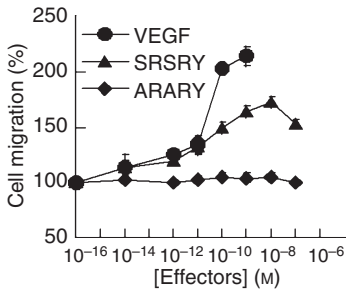

Fig. 3. The ability of soluble urokinase plasminogen activator receptor ability to promote directional endothelial cell migration is retained by the SRSRY. Human umbilical vein endothelial cells, suspended in serum-free culture medium, were allowed to migrate in Boyden chambers for 4 h at 37 °C and 5% CO_2 towards increasing concentrations of vascular endothelial growth factor $(VEGF)_{165}$, SRSRY or ARARY. The extent of cell migration was expressed as a percentage of cell migration assessed in the absence of the chemoattractant, considered as 100%. Data are the means ± standard deviations of three independent experiments performed in duplicate.

containing venous ring and sprouts with anti-CD31. This staining revealed that the 50–55% of cells were $CD31^+$. Quantification of cell sprouting was assessed by measuring the length of sprouts emerging from the venous ring (radii) and calculating, for each radius, the area of the circular segment. After 7 days, VEGF, Su-PAR and SRSRY caused increases (5.4%, 4.5% and 4.1%, respectively) in the areas of EC sprouting as compared with the control (Fig. 5). Interestingly, Su-PAR promoted cell sprouting more efficiently than SRSRY, raising the possibility that other regions of u-PAR may be involved. It would be interesting to ascertain whether the chemotactic sequence identified by Degryse *et al.* [32] in DII cooperates with the SRSRY region to enhance EC sprouting.

SRSRY elicits an angiogenic response in vivo

To test the effect of SRSRY *in vivo*, we employed the DIVAA assay, which allows quantitative assessment of angiogenesis

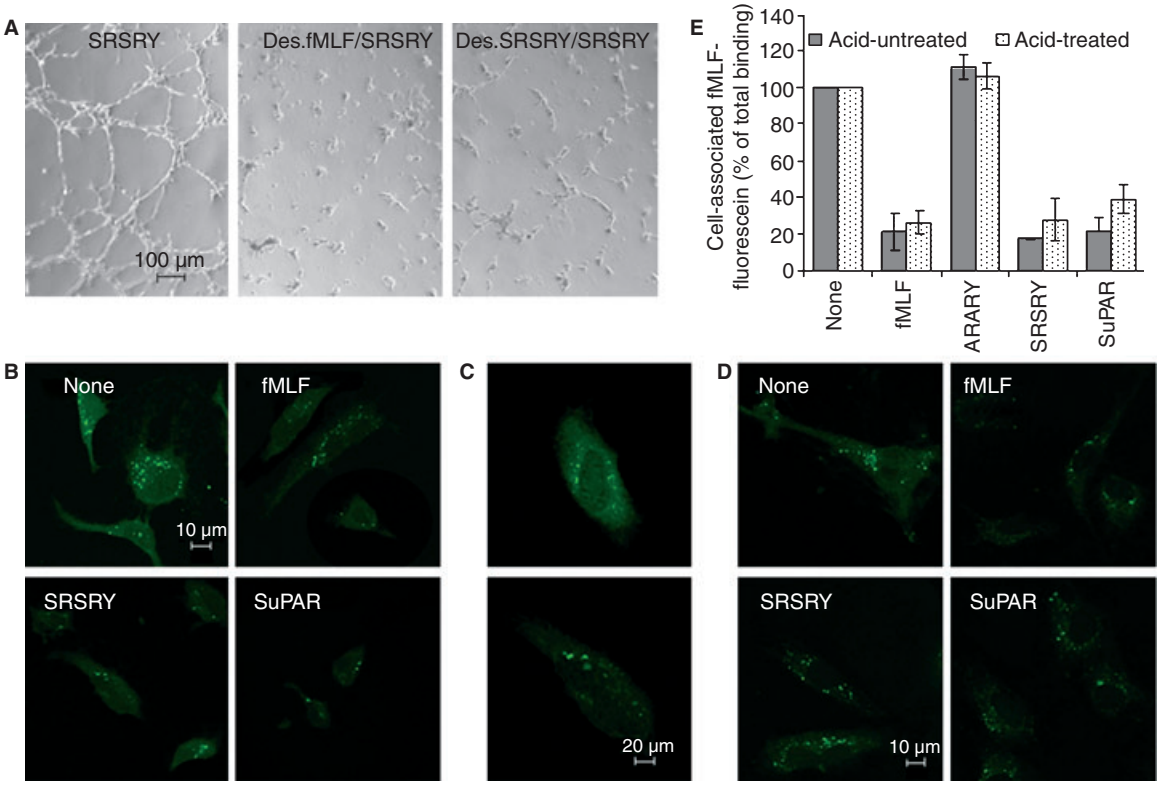

Fig. 4. Soluble urokinase plasminogen activator receptor (Su-PAR) and SRSRY stimulate rapid internalization of formyl-peptide receptor in endothelial cells. (A) Human umbilical vein endothelial cells (HUVECs) were desensitized with 100 nmol L^{-1} *N*-formyl-Nle-Leu-Phe-Nle-Tyr-Lys (fMLF) or 100 nmol L^{-1} SRSRY for 1 h at 37 °C and then seeded on matrigel-coated plates in the presence of 10 nmol L^{-1} SRSRY. Original magnifications: × 100. (B) Representative images of HUVECs grown on glass slides to semiconfluence, incubated with diluents (none), 100 nmol L^{-1} fMLF, 100 nmol L^{-1} SRSRY or 10 nmol L^{-1} Su-PAR for 60 min at 4 °C and exposed to 10 nmol L^{-1} fMLF-fluorescein for 60 min at 4 °C. Original magnification: × 630. (C) HUVECs were incubated with 10 nmol L^{-1} fMLF-fluorescein for 60 min at 4 °C and then subjected to phosphate-buffered saline (upper panel) or acid treatment (lower panel) for 5 min at room temperature. Original magnification: × 630. (D) HUVECs were incubated with diluents (none), 100 nmol L^{-1} fMLF, 100 nmol L^{-1} SRSRY or 10 nmol L^{-1} Su-PAR for 30 min at 37 °C and exposed to 10 nmol L^{-1} fMLF-fluorescein for 30 min at 37 °C. Original magnification: × 630. (E) HUVECs plated on 24-well plates, and incubated with diluents (none), 100 nmol L^{-1} fMLF, 100 nmol L^{-1} ARARY, 100 nmol L^{-1} SRSRY or 10 nmol L^{-1} SuPAR for 30 min at 37 °C, were acid-untreated or acid-treated for 5 min at room temperature and then exposed to 10 nmol L^{-1} fMLF-fluorescein for 60 min at 4 °C. Fluorimetric measurement of cell-associated fluorescence was assessed with 485-nm excitation and 535-nm emission filters. Data, expressed as a percentage of the fluorescence associated with cells exposed to fMLF-fluorescein (none), are the means ± standard deviations of three independent experiments performed in duplicate.

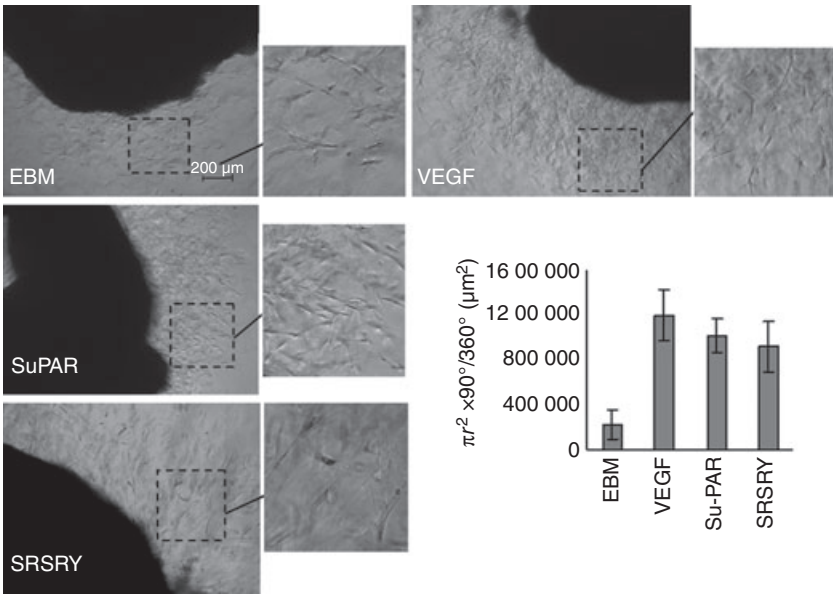

Fig. 5. Soluble urokinase plasminogen activator receptor (Su-PAR) and SRSRY promote capillary outward sprouting of human venous rings. Human saphenous vein rings of thickness 2–3 mm embedded in matrigel were incubated with 1 mL of serum-free culture medium containing diluents (Eagle Basal Medium [EBM]), 40 ng mL^{-1} vascular endothelial growth factor $(VEGF)_{165}$, 1 nmol L^{-1} Su-PAR or 10 nmol L^{-1} SRSRY for 7 days, and observed with an inverted microscope at × 50 magnification. Areas marked with dashed boxes are magnified on the right side of each panel. Photographs are representative of rings from duplicate assays. Histogram: measurement of capillary sprouting assessed by calculating the area of circular segments according to the formula πr^2 90°/360°, in which radii (r) correspond to the length of the emerging sprouts.

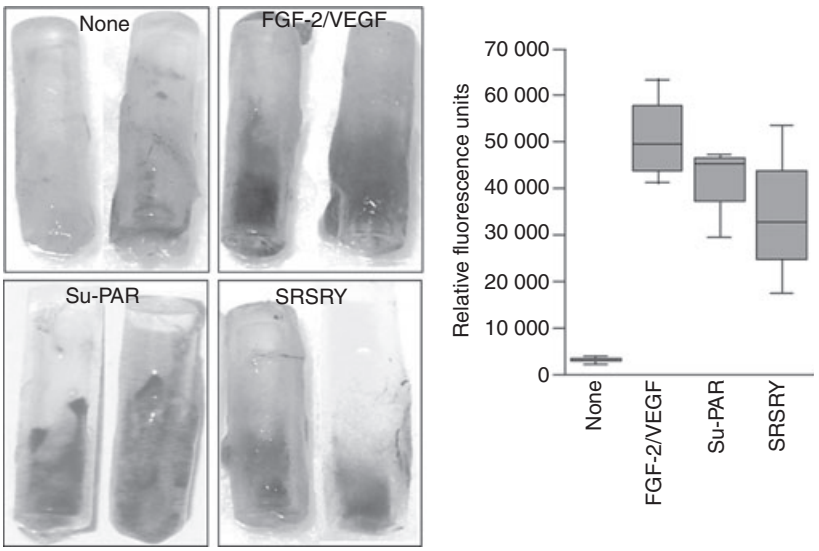

Fig. 6. Soluble urokinase plasminogen activator receptor (Su-PAR) and SRSRY promote angiogenesis *in vivo*. Matrigel-containing angioreactors loaded with diluents (none), a mixture of 12.5 ng of vascular endothelial growth factor (VEGF) and 37.5 ng of fibroblast growth factor type 2 (FGF-2), 1 nmol L^{-1} Su-PAR or 10 nmol L^{-1} SRSRY were implanted subcutaneously into the dorsal flank of eight CD1 nude mice (two angioreactors per mouse). Fifteen days after the implantation, mice were killed and angioreactors were removed. Left: macroscopic view of the resulting angioreactors in one of two experiments with similar results. Right: fluorimetric measurement of fluorescein isothiocyanate–lectin-labeled endothelial cells recovered by dispase digestion from vessels developed in matrigel-containing angioreactors. Boxplots represent data from a total of four angioreactors per sample.

in vivo. Matrigel-containing angioreactors were loaded with diluents, a mixture of VEGF and FGF-2, 1 nmol L^{-1} Su-PAR or 10 nmol L^{-1} SRSRY, and implanted into the dorsal flank of nude mice. After 15 days, capillary sprouts originating from the host vessels that invaded angioreactors were quantified by measuring fluorescence associated with ECs, following staining with FITC–lectin. As expected, VEGF and FGF-2 caused dramatic sprouting of host vessels as compared with controls (Fig. 6). Interestingly, both Su-PAR and SRSRY generated remarkably high angiogenic responses, although to different extents. Measurement of EC-associated fluorescence revealed that Su-PAR and SRSRY retained 91% and 66%, respectively,

of the fluorescence recovered by angioreactors loaded with VEGF and FGF-2 (Fig. 6). Taken together, our findings indicate that Su-PAR promotes *in vitro* and *in vivo* angiogenesis, and that this effect mainly depends on its Ser^{88}-Arg-Ser-Arg-Tyr^{92} chemotactic sequence.

Discussion

The current study demonstrates that Su-PAR promotes *in vitro* EC migration and cord-like structure formation through its Ser^{88}-Arg-Ser-Arg-Tyr^{92} sequence. We also provide evidence that Su-PAR and SRSRY can drive *ex vivo* sprouting of human primary vein rings in culture and, *in vivo,* promote a marked response in angioreactors implanted into the dorsal flank of nude mice. Remarkably, Su-PAR potency is comparable to that of VEGF, a widely recognized central factor in angiogenesis.

The role of u-PAR in angiogenesis is not unexpected, by virtue of its ability to focus urokinase activity on the cell surface. In fact, the role of u-PA in promoting angiogenesis through its surface-associated proteolytic activity is well documented [4,5]. We show here that Su-PAR may contribute to the enhancement of tube formation through SRSRY-dependent signaling in a protease-independent manner. The relevance of this observation is not obvious, considering that: (i) Su-PAR and its derived fragments are originated by shedding from the cell surface or by alternative splicing and subsequent proteolysis; and (ii) soluble forms of cleaved receptor, including the u-PARDII-DIII form, lacking the u-PA-binding domain, have been detected in tumor tissues and body fluids, and are associated with a poor prognosis [10,16–18].

Our findings show, for the first time, that u-PAR behaves as a proangiogenic factor. It promotes migration and tube formation of human ECs in a protease-independent manner. In fact, preincubation of ECs with a specific serine protease inhibitor, or with antibodies blocking the u-PA enzymatic activity, does not prevent Su-PAR-induced cord-like structure formation. Several lines of evidence support the finding that the proteolytic-independent, u-PAR-dependent proangiogenic effect mainly depends on its chemotactic Ser^{88}-Arg-Ser-Arg-Tyr^{92} sequence: (i) Su-PAR and SRSRY synthetic peptide elicit tube formation to a similar extent; (ii) $DIIDIII_{88–284}$ containing the Ser^{88}-Arg-Ser-Arg-Tyr^{92} chemotactic sequence induce cord-like structure formation, whereas $DI_{1–87}$ or $DIII_{184–284}$ does not; and (iii) both Su-PAR-triggered and SRSRY-triggered tube formation are prevented by specific u-PAR antibodies directed towards its 84–95 sequence.

Besides a role in localizing u-PA activity, the consolidated evidence assigns to u-PAR a protease-independent ability to form signaling units with integrins and FPRs [6,7,15,33].

We have previously reported that the Ser^{88}-Arg-Ser-Arg-Tyr^{92} sequence of u-PAR binds to FPR and, at high concentrations, causes FPR desensitization [12,15]. Accordingly, an excess of SRSRY, as well as of fMLF, drastically decreased the formation of cord-like structures in response to SRSRY stimulation.

In this study, we have shown that the ability of Su-PAR to trigger the formation of a capillary network of ECs involves the internalization of FPR. Cell responses to chemotactic factors are tightly controlled by a variety of desensitization/internalization mechanisms. Following agonist stimulation, FPR has been reported to translocate to lipid rafts and internalize. However, the mechanisms by which FPR may be trapped in the perinuclear recycling compartment prior to recycling to the cell surface have not been fully explored [34]. It will be interesting to ascertain whether and how FPR, upon SRSRY-triggered internalization, recycles to the EC plasma membranes.

Upon binding to FPR, SRSRY activates, with an inside-out mechanism, the vitronectin receptor in HEK-293 cells [15]. During vascularization, the $\alpha_v\beta_3$ vitronectin receptor interacts with the VEGF2 receptor to regulate migration, survival and morphogenesis of ECs [35]. It will be interesting to ascertain whether SRSRY-triggered and FPR-mediated integrin activation leading to angiogenesis may involve other transmembrane partners such as VEGFR2. It has been reported that VEGF promotes pro-u-PA activation in ECs [3]. In our experiments, Su-PAR, through its chemotactic sequence, promotes the formation of cord-like structures in less than 2 h: this effect is not caused by endogenous VEGF secretion, as it also occurs in the presence of antibodies neutralizing the biological activity of both $VEGF_{165}$ and $VEGF_{121}$ [27].

An apparently conflicting finding has been reported by Jo *et al.* [36], showing that Su-PAR may inhibit tumor progression and invasion. However, this effect may be attributable to its ability to function as a scavenger for u-PA, thus inhibiting its proteolytic activity. It is reasonable to hypothesize that regulation of Su-PAR secretion and localization may alter the functional output in different ways, so that the net *in vivo* result would be difficult to predict. Our findings, together with the increased expression level of Su-PAR in cancer patients, highlight the possibility that Su-PAR-dependent stimulation of angiogenesis may occur during tumor progression *in vivo*. Although the peptide SRSRY is not found *in vivo*, the notion that this sequence is active in signaling while in the isolated form suggests an important, additional role of u-PAR in angiogenesis. Our results suggest a new scenario that may occur during tumor progression: increased levels of u-PAR on tumor cell surfaces favor u-PAR shedding in the extracellular milieu, or Su-PAR may be generated by an alternative splicing mechanism; Su-PAR, similarly to ligand-engaged GPI-anchored u-PAR, may undergo a conformational change that uncovers the chemotactic region that, in turn, could trigger tumor-associated neoangiogenesis by a mechanism that involves formyl-peptide and vitronectin receptors. Our hypothesis is in agreement with that of Jo *et al.* [37], who found that non-invasive HEK-293 cells acquire, upon transfection with u-PAR, the ability to metastasize independently of u-PA.

The finding that u-PAR can exist in soluble and cleaved forms, its relatively low level in normal, quiescent tissues and its proangiogenic role confirm that u-PAR is an important target for the treatment of solid tumors. In this respect, different

approaches have been used to disrupt its interactions with u-PA, integrins or FPRs [22,32,38,39].

A relationship between long-term inflammation and a predisposition for the development of cancer has been suggested [40]. In this respect, it is noteworthy that u-PAR is involved in acute and chronic inflammation as well as in chronic degenerative vascular processes [41]. In the future, the ability of SRSRY-derived compounds to promote the formation of new collateral vessels in ischemic tissues could be tested. On the contrary, antagonists of the Ser^{88}-Arg-Ser-Arg-Tyr^{92} sequence are expected to disrupt the signals, enabling vascular cells to respond to the tumor-associated extracellular environment and to promote tumor-induced angiogenesis.

Addendum

K. Bifulco: tube formation and aortic ring experiments, data Collection and image analysis; I. Longanesi-Cattani: Cell migration and aortic ring experiments, data collection and immunofluorescence; M. Gala: *in vivo* experiments; G. Di Carluccio: fluorimetric experiments; M.T. Masucci: SuPAR production and quantification; V. Pavone: mass spectrometry analysis and interpretation of the results; L. Lista: synthesis of peptides, HPLC; C. Arra: *in vivo* experiments, analysis and interpretation of the results; M.P. Stoppelli: analysis and interpretation of the results and writing the article; M.V. Carriero: conception and design, analysis and interpretation of the results, and writing the article.

Acknowledgements

LB6 and LB6/hSu-PAR cells were a gift of F. Blasi (DIBIT, Milan, Italy). The rabbit anti-u-$PAR_{84–95}$ polyclonal antibody was a gift from P. Ragno (University of Salerno, Italy). This work was supported by the Italian Ministry of Health (FSN2007) and by the ESF Eurocore Project, Contract no. LSHC-CT-2003-503297.

Disclosure of Conflict of Interests

The authors state that they have no conflict of interest.

Supporting Information

Additional Supporting Information may be found in the online version of this article:

Figure S1. Human umbilical vein endothelial cells (HUVECs) were exposed to 10 nmol L^{-1} *N*-formyl-Nle-Leu-Phe-Nle-Tyr-Lys (fMLF)-fluorescein for 30 min at 37 °C, and visualized with a Zeiss 510META LSM microscope.

Please note: Wiley-Blackwell are not responsible for the content or functionality of any supporting materials supplied by the authors. Any queries (other than missing material) should be directed to the corresponding author for the article.

References

1 Carmeliet P. Angiogenesis in health and disease. *Nat Med* 2003; **9**: 653–60.
2 Mahabeleshwar GH, Feng W, Reddy K, Plow EF, Byzova TV. Mechanisms of integrin–vascular endothelial growth factor receptor cross-activation in angiogenesis. *Circ Res* 2007; **101**: 570–80.
3 Prager GW, Breuss JM, Steurer S, Mihaly J, Binder BR. Vascular endothelial growth factor (VEGF) induces rapid prourokinase (pro-uPA) activation on the surface of endothelial cells. *Blood* 2004; **103**: 955–6.
4 Binder BR, Mihaly J, Prager GW. uPAR–uPA–PAI-1 interactions and signalling: a vascular biologist's view. *Thromb Haemost* 2007; **97**: 336–42.
5 Pepper MS. Role of the matrix metalloproteinase and plasminogen activator–plasmin systems in angiogenesis. *Arterioscler Thromb Vasc Biol* 2001; **21**: 1104–17.
6 Blasi F, Carmeliet P. uPAR: a versatile signaling orchestrator. *Nat Rev Mol Cell Biol* 2002; **3**: 932–43.
7 Smith HW, Marshall CJ. Regulation of cell signalling by uPAR. *Nat Rev Mol Cell Biol* 2010; **11**: 23–36.
8 Prager GW, Mihaly J, Brunner PM, Koshelnick Y, Hoyer-Hansen G, Binder BR. Urokinase mediates endothelial cell survival via induction of the X-linked inhibitor of apoptosis protein. *Blood* 2009; **113**: 1383–90.
9 Ploug M, Rønne E, Behrendt N, Jensen AL, Blasi F, Danø K. Cellular receptor for urokinase plasminogen activator. Carboxyl-terminal processing and membrane anchoring by glycosyl-phosphatidylinositol. *J Biol Chem* 1991; **266**: 1926–33.
10 Rasch MG, Lund IK, Almasi CE, Hoyer-Hansen G. Intact and cleaved uPAR forms: diagnostic and prognostic value in cancer. *Front Biosci* 2008; **13**: 6752–62.
11 Ploug M, Ellis V. Structure–function relationships in the receptor for urokinase-type plasminogen activator. Comparison to other members of the Ly-6 family and snake venom alpha-neurotoxins. *FEBS Lett* 1994; **349**: 163–8.
12 Selleri C, Montuori N, Ricci P, Visconte V, Baiano A, Carriero MV, Rotoli B, Rossi G, Ragno P. In vivo activity of the cleaved form of soluble urokinase receptor: a new hematopoietic stem/progenitor cell mobilizer. *Cancer Res* 2006; **66**: 10885–990.
13 Resnati M, Guttinger M, Valcamonica S, Sidenius N, Blasi F, Fazioli F. Proteolytic cleavage of the urokinase receptor substitutes for the agonist-induced chemotactic effect. *EMBO J* 1996; **15**: 1572–82.
14 Resnati M, Pallavicini I, Wang JM, Oppenheim J, Serhan CN, Romano M, Blasi F. The fibrinolytic receptor for urokinase activates the G protein-coupled chemotactic receptor FPRL1/LXA4R. *Proc Natl Acad Sci USA* 2002; **99**: 1359–64.
15 Gargiulo L, Longanesi-Cattani I, Bifulco K, Franco P, Raiola R, Campiglia P, Grieco P, Peluso G, Stoppelli MP, Carriero MV. Cross-talk between fMLP and vitronectin receptors triggered by urokinase receptor-derived SRSRY peptide. *J Biol Chem* 2005; **280**: 25225–32.
16 Sidenius N, Blasi F. The urokinase plasminogen activator system in cancer: recent advances and implication for prognosis and therapy. *Cancer Metastasis Rev* 2003; **22**: 205–22.
17 Henic E, Borgfeldt C, Christensen IJ, Casslén B, Høyer-Hansen G. Cleaved forms of the urokinase plasminogen activator receptor in plasma have diagnostic potential and predict postoperative survival in patients with ovarian cancer. *Clin Cancer Res* 2008; **14**: 5785–93.
18 Shariat SF, Roehrborn CG, McConnell JD, Park S, Alam N, Wheeler TM, Slawin KM. Association of the circulating levels of the urokinase system of plasminogen activation with the presence of prostate cancer and invasion, progression, and metastasis. *J Clin Oncol* 2007; **25**: 349–55.
19 Llinas P, Le Du MH, Gårdsvoll H, Danø K, Ploug M, Gilquin B, Stura EA, Ménez A. Crystal structure of the human urokinase

plasminogen activator receptor bound to an antagonist peptide. *EMBO J* 2005; **24**: 1655–63.
20 Barinka C, Parry G, Callahan J, Shaw DE, Kuo A, Bdeir K, Cines DB, Mazar A, Lubkowski J. Structural basis of interaction between urokinase-type plasminogen activator and its receptor. *J Mol Biol* 2006; **363**: 482–95.
21 Furlan F, Orlando S, Laudanna C, Resnati M, Basso V, Blasi F, Mondino A. The soluble D2D3(88–274) fragment of the urokinase receptor inhibits monocyte chemotaxis and integrin-dependent cell adhesion. *J Cell Sci* 2004; **117**: 2909–16.
22 Carriero MV, Longanesi-Cattani I, Bifulco K, Maglio O, Lista L, Barbieri A, Votta G, Masucci MT, Arra C, Franco R, De Rosa M, Stoppelli MP, Pavone V. Structure-based design of an urokinase-type plasminogen activator receptor-derived peptide inhibiting cell migration and lung metastasis. *Mol Cancer Ther* 2009; **9**: 2708–17.
23 Arnaoutova I, Kleinman HK. In vitro angiogenesis: endothelial cell tube formation on gelled basement membrane extract. *Nat Protoc* 2010; **5**: 628–35.
24 Masucci MT, Pedersen N, Blasi F. A soluble, ligand binding mutant of the human urokinase plasminogen activator receptor. *J Biol Chem* 1991; **266**: 8655–8.
25 Carriero MV, Franco P, Del Vecchio S, Massa O, Botti G, D'Aiuto G, Stoppelli MP, Salvatore M. Tissue distribution of soluble and receptor-bound urokinase in human breast cancer using a panel of monoclonal antibodies. *Cancer Res* 1994; **54**: 5445–54.
26 Yang S, Graham J, Kahn JW, Schwartz EA, Gerritsen ME. Functional roles for PECAM-1 (CD31) and VE-cadherin (CD144) in tube assembly and lumen formation in three-dimensional collagen gels. *Am J Pathol* 1999; **155**: 887–95.
27 Baroni A, Donnarumma G, Paoletti I, Longanesi-Cattani I, Bifulco K, Tufano MA, Carriero MV. Antimicrobial human beta-defensin-2 stimulates migration, proliferation and tube formation of human umbilical vein endothelial cells. *Peptides* 2009; **30**: 267–72.
28 Montuori N, Carriero MV, Salzano S, Rossi G, Ragno P. The cleavage of the urokinase receptor regulates its multiple functions. *J Biol Chem* 2002; **277**: 46932–9.
29 Carriero MV, Del Vecchio S, Franco P, Potena M, Botti G, Stoppelli MP, Salvatore M. Vitronectin binding to urokinase receptor in human breast cancer. *Clin Cancer Res* 1997; **3**: 1299–308.
30 Guedez L, Rivera AM, Salloum R, Miller ML, Diegmueller JJ, Bungay PM, Stetler-Stevenson WG. Quantitative assessment of angiogenic responses by the directed in vivo angiogenesis assay. *Am J Pathol* 2003; **162**: 1431–9.
31 Perez DM, Karnik SS. Multiple signaling states of G-protein-coupled receptors. *Pharmacol Rev* 2005; **57**: 147–61.
32 Degryse B, Resnati M, Czekay RP, Loskutoff DJ, Blasi F. Domain 2 of the urokinase receptor contains an integrin-interacting epitope with intrinsic signaling activity: generation of a new integrin inhibitor. *J Biol Chem* 2005; **280**: 24792–803.
33 Kjaergaard M, Hansen LV, Jacobsen B, Gardsvoll H, Ploug M. Structure and ligand interactions of the urokinase receptor (uPAR). *Front Biosci* 2008; **13**: 5441–61.
34 Rabiet MJ, Huet E, Boulay F. The N-formyl peptide receptors and the anaphylatoxin C5a receptors: an overview. *Biochimie* 2007; **89**: 1089–106.
35 Somanath PR, Malinin NL, Byzova TV. Cooperation between integrin alphavbeta3 and VEGFR2 in angiogenesis. *Angiogenesis* 2009; **12**: 177–85.
36 Jo M, Thomas KS, Wu L, Gonias SL. Soluble urokinase-type plasminogen activator receptor inhibits cancer cell growth and invasion by direct urokinase-independent effects on cell signaling. *J Biol Chem* 2003; **278**: 46692–8.
37 Jo M, Takimoto S, Montel V, Gonias SL. The urokinase receptor promotes cancer metastasis independently of urokinase-type plasminogen activator in mice. *Am J Pathol* 2009; **175**: 190–200.
38 Carriero MV, Franco P, Vocca I, Alfano D, Longanesi-Cattani I, Bifulco K, Mancini A, Caputi M, Stoppelli MP. Structure, function and antagonists of urokinase-type plasminogen activator. *Front Biosci* 2009; **14**: 3782–94.
39 Bifulco K, Longanesi-Cattani I, Gargiulo L, Maglio O, Cataldi M, De Rosa M, Stoppelli MP, Pavone V, Carriero MV. An urokinase receptor antagonist that inhibits cell migration by blocking the formyl peptide receptor. *FEBS Lett* 2008; **582**: 1141–6.
40 Dranoff G. Cytokines in cancer pathogenesis and cancer therapy. *Nat Rev Cancer* 2004; **4**: 11–22.
41 Chavakis T, Kanse SM, May AE, Preissner KT. Haemostatic factors occupy new territory: the role of the urokinase receptor system and kininogen in inflammation. *Biochem Soc Trans* 2002; **30**: 168–73.